International Journal of Biology and Life Sciences
ISSN: 2957-9511 | Vol. 12, No. 2, 2025

The Usage of Electrospinning to Prepare Chitosan Fiber Films to Replace Traditional Sanitary Napkin Materials

Yinan Gong *

Shanghai Foreign Language Academy, Shanghai, China
*** Corresponding author Email:** gongyinan@yandex.com

Abstract: Conventional disposable sanitary pads are predominantly plastic-based and pose environmental and potential health risks. This study explores biodegradable alternatives by electrospinning chitosan (CS)/polyvinyl alcohol (PVA) blend nanofibrous membranes under three processing conditions, followed by characterization via scanning electron microscopy (SEM), water contact angle, and water uptake tests. Reducing the feed rate and slightly increasing the tip-to-collector distance markedly improved fiber continuity and pore network formation. The best-performing sample (Sample 3: 15% PVA1750, 0.1 $mL \cdot h^{-1}$, 10 cm) exhibited a continuous, uniform, and defect-minimized mesh with the strongest hydrophilicity (contact angle 23.22° ± 5.86°) and the highest water uptake (~1300%), outperforming Sample 1 (~375%) and Sample 2 (~414%), and greatly exceeding a hydrophobic PVDF control (~71%). These results indicate that electrospun CS/PVA nanofibers combine high absorbency with strong wettability and are promising candidates to replace plastic absorbent layers in sanitary pads. Limitations include relatively small specimen dry masses leading to larger relative errors and a non-exhaustive parameter space. Future work will employ orthogonal/response-surface designs and crosslinking/surface modifications, alongside mechanical, breathability, antibacterial, and biocompatibility evaluations to advance material readiness.

Keywords: Chitosan; Polyvinyl Alcohol; Electrospinning; Nanofibers; Contact Angle; Water Uptake; Sanitary Pads.

1. Introduction

In modern society, traditional disposable sanitary napkins are widely used due to their convenience and good absorbency. However, the environmental threats and potential health hazards that they pose during disposal have gradually drawn the public's attention. The main materials of disposable sanitary napkins usually contain over 90% plastic, including packaging, back sheet, wings, adhesive layers, etc. Each napkin even contains as much plastic as four supermarket plastic bags [1]. In the UK, over 200,000 tons of such products are generated annually, with over 80% being disposed of through landfill or incineration. During incineration, if the temperature is below 800 degrees Celsius, toxic gases such as dioxins will be released [2], polluting the air and posing a threat to human health. Landfill disposal will occupy a large amount of land, and the degradation period of disposable sanitary napkins can be as long as 500 to 800 years, far exceeding that of general waste [3]. If these plastic products are flushed down the drain or thrown into rivers or seas, they will damage the aquatic ecosystem, form microplastic pollution, and become the main cause of sewage system blockages.

The materials of traditional sanitary napkins usually use bleached wood pulp, which contains dioxins and volatile organic compounds (VOCs), such as styrene and trichloromethane, which may be absorbed by the human body through the skin or mucous membranes, thereby potentially affecting the reproductive system or development. Long-term exposure may also cause ovarian cancer or damage the immune system [4]. In addition, sanitary napkins often contain preservatives that are not clearly listed but are irritating or allergenic, which may cause contact dermatitis and other problems, posing a threat to women's health.

Given the environmental burden and potential harm to human health caused by traditional sanitary napkins during disposal, this project aims to explore female hygiene products based on degradable and highly biocompatible materials. If degradable fiber films can achieve water absorption and blood adsorption functions, they may be able to replace traditional materials, thereby reducing plastic pollution and minimizing the damage of chemicals to the human body.

This project uses chitosan as the main raw material for the experiment. Chitosan is a natural cationic polysaccharide obtained by partial deacetylation of chitin. Chitin is the second most abundant polysaccharide in nature after cellulose, mainly found in the shells of shrimp, crab, lobster, and other crustaceans, as well as in the exoskeletons of insects [5]. Industrial production can batch prepare chitosan from marine waste through processes such as acid decalcification, alkaline deproteinization, and deacetylation. Thus, using chitosan as a raw material can achieve the conditions of being renewable, widely available, and relatively low-cost, as shown in Figure. 1.

Chitosan electrospun nanofibers have become a research hotspot in recent years due to their biodegradability, biocompatibility, antibacterial properties, and coagulation-promoting capabilities, and they have been widely studied for applications in wound dressings, tissue engineering scaffolds, drug-controlled release, filtration membranes, and other biomedical and filtration fields [7] . Thus, chitosan nanofibers have great potential for application in multiple fields. This paper will explore the formation conditions and properties of the spun films based on electrospinning technology and the biodegradability and biocompatibility of chitosan using the research results.

Polyvinyl alcohol (PVA) is a water-soluble synthetic polymer with excellent electrospun properties, biocompatibility, and mechanical properties, and is widely used in medical materials, drug-controlled release, and degradable films.

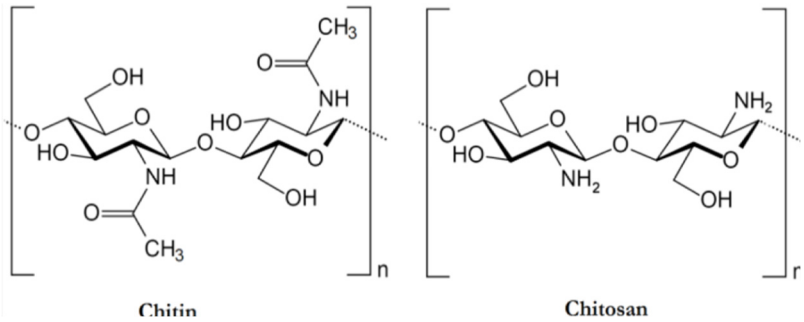


Figure 1. Molecular formulas of chitosan and chitin (Younes, I., & Rinaudo, M. 2015)

As a polymer with good spinning properties, it can effectively assist in the formation of chitosan (CS) fibers. According to research, the formation of hydrogen bonds between the molecular chains of PVA and CS reduces the entanglement threshold between CS chains [8]. Therefore, the mixing of PVA and CS can significantly enhance the fiber-forming ability of the solution, making it less likely to have defects such as breaks or bead lines during electrospinning, and generating more continuous, uniform, and bead-free nanofiber structures.

2. Raw Materials

Chitosan (CS); Polyvinyl Alcohol (PVA) 1750; Polyvinyl Alcohol (PVA) 1788； 90% acetic acid aqueous solution; Distilled water

Experimental instruments

Electrospinning machine, Yunfan (Tianjin) Instrument Co., Ltd., specification model: YFSP-T. Scanning electron microscope (SEM), Hitachi Corporation of Japan, specification model: S-4800. Contact angle measuring instrument, Defer Company of Germany, instrument model: OCA15EC.

Experimental procedures

Sample 1: 10% PVA1788, pump head injection speed 0.2mL/h

1. Use an electronic scale to weigh 1.0 g of 1788PVA powder

2. Take one vial, dissolve 1.0 g of PVA1788 powder in 9 mL of 90°C water, and place it in a 90˚C constant temperature water bath until the PVA solution is completely dissolved

3. Use a 10 mL graduated cylinder to measure 4.5 mL of 80% acetic acid

4. Use an electronic scale to weigh 0.5 g of CS powder, mix it with the acetic acid

5. Insert a magnet, use a magnetic stirrer to ensure complete dissolution

6. Take out one vial, mix 6 mL of PVA1788 with 1 mL of CS solution, stir at room temperature for 6 hours to obtain the spinning solution

Film preparation

7. Take a syringe, take in 3 mL of the raw solution, connect a metal needle above the syringe, and remove the air bubbles in the syringe

8. Place the syringe in the spinning chamber, set the spinning conditions: spinning distance 8 cm; environmental temperature 25˚C; humidity 60%; pump speed 0.2 mL/h; Working voltage 20 kV

9. Place appropriate tin foil in front of the pump head to collect the sample

10. Connect the high-voltage power supply, start the spinning machine, stop after spinning for 20 minutes, and obtain the sample

Sample 2: 15% PVA1750, pump speed 0.2 mL/h

11. Use an electronic scale to weigh 1.5 g of 1750PVA powder

12. Take one vial, dissolve 1.5 g of PVA1750 powder in 13.5 mL of water, place it in a 90˚C constant temperature water bath, and stir until completely dissolved until the PVA solution is completely dissolved

13. Take out one vial, mix 6 mL of PVA1750 with 1 mL of CS solution, stir at room temperature for 6 hours to obtain the spinning solution

Film preparation

14. Take a syringe, take in 3 mL of the raw solution, connect a metal needle above the syringe, and remove the air bubbles in the syringe

15. Place the syringe in the spinning chamber, set the spinning conditions: spinning distance 8 cm; environmental temperature 25˚C; humidity 60%; pump head injection speed 0.2 mL/h

16. Place appropriate tin foil in front of the pump head to collect the sample

17. Connect the high-voltage power supply, start the spinning machine, stop after spinning for 20 minutes, and obtain the sample

Sample 3: 15% PVA1750, pump speed 0.1 mL/h

18. Take out one vial, mix 6 mL of PVA1750 with 1 mL of CS solution, stir at room temperature for 6 hours, to obtain the spinning solution

Film preparation

19. Take a syringe, take in 3 mL of the raw solution, connect a metal needle above the syringe, and remove the air bubbles in the syringe

20. Place the syringe in the spinning chamber, set the spinning conditions: spinning distance 10 cm; environmental temperature 25˚C; humidity 60%; pump speed 0.1 mL/h; Working voltage 20 kV

21. Place appropriate tin foil in front of the pump head to collect the sample

22. Connect the high-voltage power supply, start the spinning machine, stop after spinning for 30 minutes, and obtain the sample

3. Sample testing

Scanning electron microscope examination

Scanning Electron Microscopy (SEM) is a detection method that uses a focused electron beam to scan the surface of a sample. It can form images based on the signals generated

by the interaction between electrons and materials, thereby obtaining information about the microscopic structure and morphology of the material's surface. For fiber membranes prepared by electrospinning, SEM can directly observe the diameter, continuity, surface smoothness, and pore structure of the fibers, thereby analyzing the relationship between film formation quality and water absorption performance. An ideal alternative material for sanitary napkins should present a continuous, uniform, and defect-free nanofiber network under the scanning electron microscope, providing sufficient capillary channels and specific surface area, thereby enhancing liquid absorption and diffusion capabilities.

Sample 1: 10% PVA1788, pump speed 0.2 mL/h

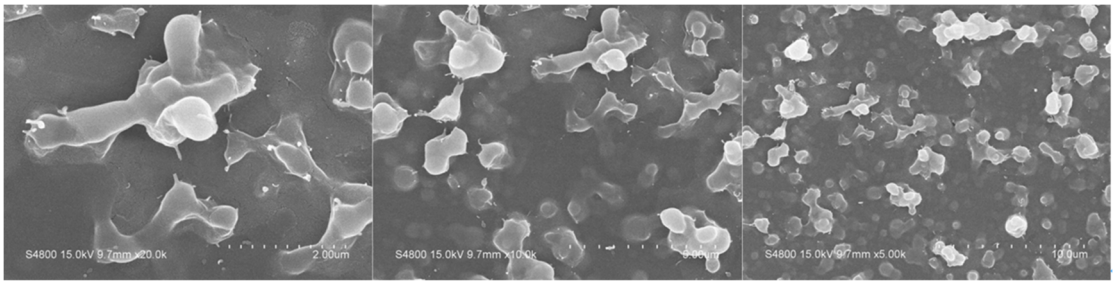


Figure 2. 10% PVA1788, pump speed 0.2 mL/h, SEM (The magnification of the pictures is 20,000 times, 10,000 times, and 5,000 times respectively.)

As shown in Figure 2, the SEM scan results show that the fibers failed to form a clear and continuous network structure. In the spun products, there are a large number of irregular short fibers and a small amount of aggregated blocks. Thus, the connectivity between the fibers in sample 1 is poor, and the pore network is discontinuous. This indicates that under the formulation and process parameters of this sample, the solution viscosity or the degree of molecular chain entanglement did not reach the threshold required for steady-state spinning. The jet is prone to breakage during the stretching process and causes droplet solidification, thus unable to form a uniform and continuous nanofiber network.

Sample 2: 15% PVA1750, pump speed 0.2 mL/h

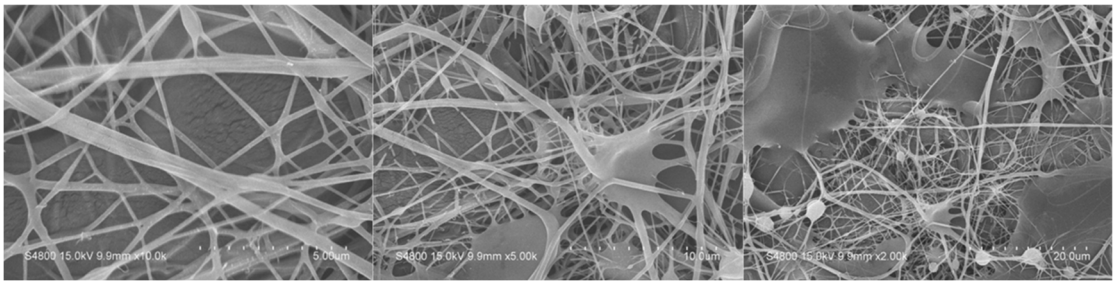


Figure 3. 15% PVA1750, pump speed 0.2 mL/h, SEM (The magnification of the pictures is 10,000 times, 5,000 times, and 2,000 times respectively.)

As shown in Figure 3, after reducing the pumping speed and appropriately increasing the spinning distance, SEM images showed that the fibers became more continuous, smoother, and the mesh structure was more complete. The spherical particles were significantly reduced, and a uniform porous network was formed between the fibers. This structure can increase the specific surface area and the number of capillary channels, thereby significantly enhancing the film's ability to absorb and diffuse liquids. Thus, it can be concluded that reducing the pumping speed and elongating the spinning distance is beneficial for the jet to have sufficient time to be stretched by the electric field, resulting in uniform fibers.

Sample 3: 15% PVA1750, pump head injection speed 0.1 mL/h

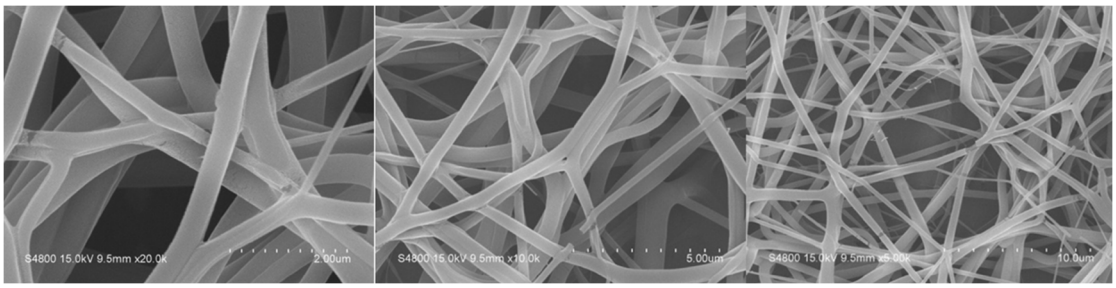


Figure 4. 15% PVA1750, pump head injection speed 0.1 mL/h SEM (The magnification of the pictures is 20,000 times, 10,000 times, and 5,000 times respectively.)

As shown in Figure 3, after reducing the pumping speed and appropriately increasing the spinning distance, SEM images showed that the fibers became more continuous, smoother, and the mesh structure was more complete. The spherical particles were significantly reduced, and a uniform porous network was formed between the fibers. This structure can increase the specific surface area and the number of capillary channels, thereby significantly enhancing the film's ability to absorb and diffuse liquids.

Contact angle measurement

Contact angle measurement is an important method for evaluating the wetting properties of material surfaces. The principle is to drop a droplet of liquid onto the sample surface and then measure the angle between the droplet and the sample surface using the principle of optical imaging. This allows for the determination of the material's hydrophilic or hydrophobic properties. The smaller the contact angle, the more the droplet spreads on the material surface, indicating better hydrophilicity. On the other hand, a larger contact angle means the droplet remains spherical, indicating a more hydrophobic surface. For absorbent materials that are good at absorbing liquids, the ideal result should be a smaller contact angle to facilitate the rapid diffusion and absorption of liquids.

Sample 1: 10% PVA1788, pump speed 0.2 mL/h

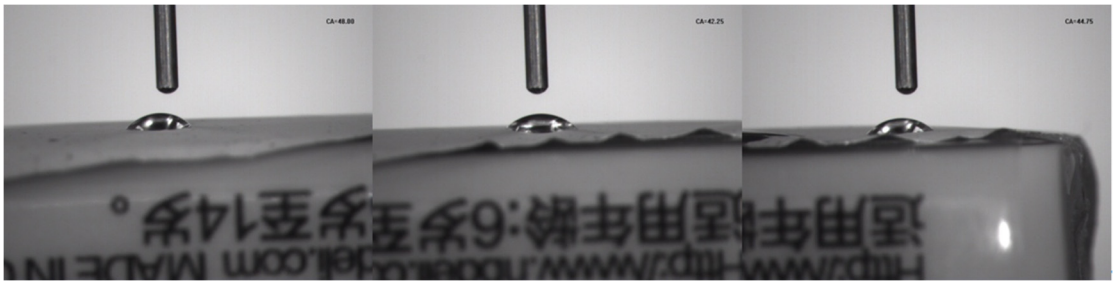


Figure 5. 10% PVA1788, pump speed 0.2 mL/h (contact angle 1, contact angle 2, contact angle 3)

After testing, the three contact angle measurements of sample 10% PVA1788 with a pump speed of 0.2 mL/h were 48.00˚, 42.25˚, and 44.75˚ respectively. From this, it can be known that the average contact angle of this sample is:

$$Contact\ angle = \frac{48.00^{\circ} + 42.25^{\circ} + 44.75^{\circ}}{3} \approx 45.00^{\circ}$$

$$Uncertainty = \frac{48.00-42.25}{2} \approx 3^{\circ}$$

Therefore, the contact angle of sample 1 is: $45^{\circ} \pm 3^{\circ}$

Sample 2: 15% PVA1750, pump head injection speed 0.2 mL/h

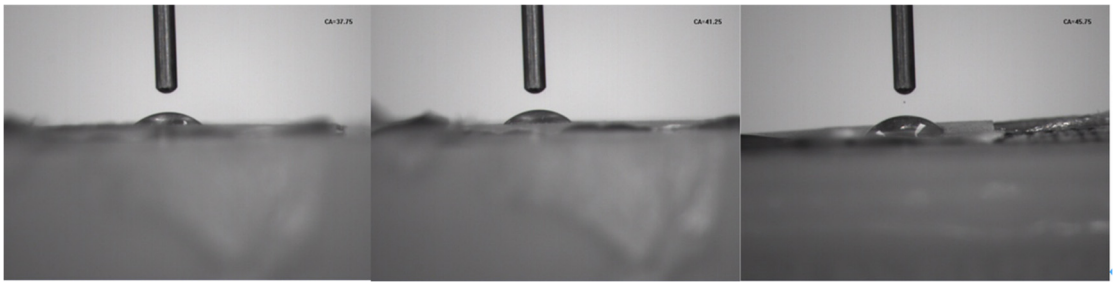


Figure 6. 15% PVA1750, pump speed 0.2 mL/h (contact angle 1, contact angle 2, contact angle 3)

After testing, the three contact angle measurements of sample 10% PVA1788 with a pump speed of 0.2 mL/h were 48.00˚, 42.25˚, and 44.75˚ respectively. From this, it can be known that the average contact angle of this sample is:

$$Contact\ angle = \frac{41.25^{\circ} + 45.75^{\circ} + 37.45^{\circ}}{3} \approx 41.48^{\circ}$$

$$Uncertainty = \frac{45.75^{\circ}-37.45^{\circ}}{2} \approx 4^{\circ}$$

Therefore, the contact angle of sample 2 is: $42^{\circ} \pm 4^{\circ}$

Sample 3: 15% PVA1750, pump head injection speed 0.1 mL/h

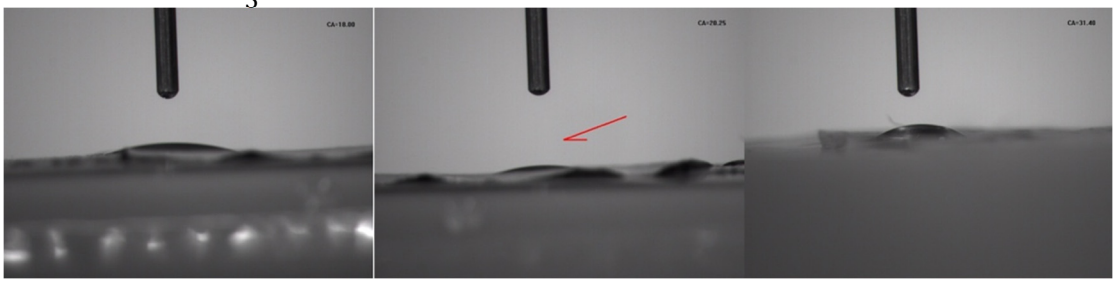


Figure 7. 15% PVA1750, pump speed 0.1 mL/h (contact angle 1, contact angle 2, contact angle 3)

After testing, the three contact angle measurements of sample 10% PVA1788 with a pump speed of 0.2 mL/h were 18.00˚, 31.40˚, and 20.25˚ respectively. From this, it can be known that the average contact angle of this sample is:

$$Contact\ angle = \frac{18.00^{\circ} + 31.40 + ^{\circ}20.25^{\circ}}{3} \approx 23.22^{\circ}$$

$$Uncertainty = \frac{31.40^{\circ}-18.00^{\circ}}{2} \approx 7^{\circ}$$

Therefore, the contact angle of sample 3 is: $23^{\circ} \pm 7^{\circ}$

As shown in Figure 5-7, The contact angles of all three samples were below 90°, indicating that all the samples had a certain degree of hydrophilicity. Among them, the contact angle of sample 3, which was 23.22° ± 5.86°, was the smallest among the three samples. It showed significant differences from the contact angles of sample 1 (45.00° ± 2.35°) and sample 2 (41.48° ± 3.39°), suggesting that it had the strongest hydrophilicity. This is consistent with the continuous porous and uniform fiber structure observed in the SEM, indicating that a higher surface area and more capillary channels can significantly reduce the surface contact angle and enhance liquid diffusion and absorption.

Water absorption test

The water absorption test is used to evaluate the material's ability to absorb water when in contact with a liquid, reflecting its efficiency in absorbing menstrual blood or other body fluids in hygiene products. The test method is as follows: Cut three samples to the same size respectively. Weigh them using an electronic scale and record the m_{dry}. Then, take three beakers, add 3 mL of water to each, immerse the samples for 3 minutes, allowing them to fully absorb water before removing them, measure the wet weight m_{wet}, and finally calculate the water absorption rate using the formula:

Water absorption rate(R)=$\frac{m_{dry}-m_{wet}}{m_{dry}} \times 100\%$

Uncertainty of Water absorption rate (ΔR) =$\sqrt{(\frac{100 \cdot m_{wet}}{m_{dry}^2} \cdot \Delta m)^2 + (\frac{100}{m_{dry}} \cdot \Delta m)^2}$

The higher the water absorption rate, the stronger the water absorption ability of the material. The ideal result should be that the water absorption rate is significantly higher than that of the hydrophobic control group, and it should have a small relative error.

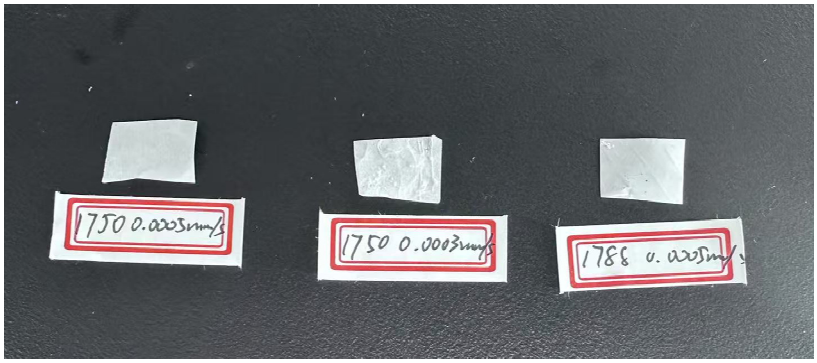


Figure 8. Right: 10% PVA1788, pump speed 0.2 mL/h
Middle: 15% PVA1750, pump speed 0.2 mL/h
Left: 15% PVA1750, pump speed 0.1 mL/h

Sample 1: 10% PVA1788, pump speed 0.2 mL/h



Figure 9. 10% PVA1788, pump speed 0.2 mL/h, before water absorption



Figure 10. 10% PVA1788, pump speed 0.2 mL/h, after water absorption

As shown in Figure 9, 10, by weighing with an electronic scale, the mass of the sample before absorbing water was 0.008g, and the mass after absorbing water was 0.038g. The error of the electronic scale is 0.001g. Therefore, the water absorption rate of this sample is:

$$R_1 = \frac{0.038 - 0.008}{0.008} \times 100\% = 375.00\%$$

$$\Delta R_1 = \sqrt{(\frac{100 \cdot 0.038}{0.008^2} \times 0.001)^2 + (\frac{100}{0.008} \times 0.001)^2} \approx 60.7\%$$

$$R_1 = 375.0\% \pm 60.7\%$$

Sample 2: 15% PVA1750, pump speed 0.2 mL/h

As shown in Figure 11-12, by weighing with an electronic scale, the mass of the sample before absorbing water was 0.007g, and the mass after absorbing water was 0.036g. Thus, it can be concluded that the water absorption rate of this sample is:

$$R_2 = \frac{0.036 - 0.007}{0.007} \times 100\% = 414.3\%$$

$$\Delta R_2 = \sqrt{(\frac{100 \cdot 0.036}{0.007^2} \times 0.001)^2 + (\frac{100}{0.007} \times 0.001)^2} \approx 74.8\%$$

$$R_2 = 414.3\% \pm 74.8\%$$

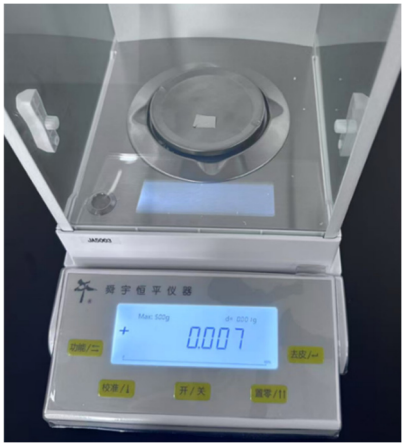


Figure 11. 15% PVA1750, pump speed 0.2 mL/h, before water absorption



Figure 12. 15% PVA150, pump speed 0.2 mL/h, after water absorption

Sample 3: 15% PVA1750, pump head injection speed 0.1 mL/h



Figure 13. 15% PVA1750, pump speed 0.1 mL/h, before water absorption

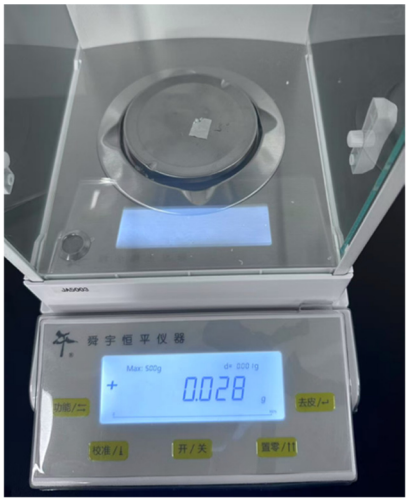


Figure 14. 15% PVA150, pump speed 0.1 mL/h, after water absorption

As shown in Figure 13 and 14, by weighing with an electronic scale, the mass of the sample before absorbing water was 0.002g, and the mass after absorbing water was 0.028g. Thus, it can be concluded that the water absorption rate of this sample is

$$R_3 = \frac{0.028 - 0.002}{0.002} \times 100\% = 1300.00\%$$

$$\Delta R_3 = \sqrt{\left(\frac{100 \cdot 0.028}{0.002^2} \times 0.001\right)^2 + \left(\frac{100}{0.002} \times 0.001\right)^2} \approx 701.8\%$$

$$R_3 = 1300.0\% \pm 701.8\%$$

PVDF electrospun membrane (hydrophobic)

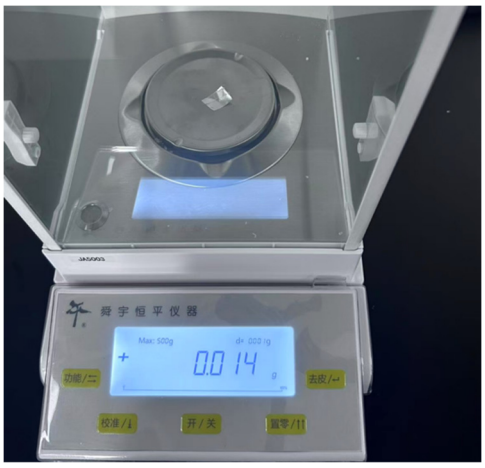


Figure 15. PVDF electrospun membrane before water absorption

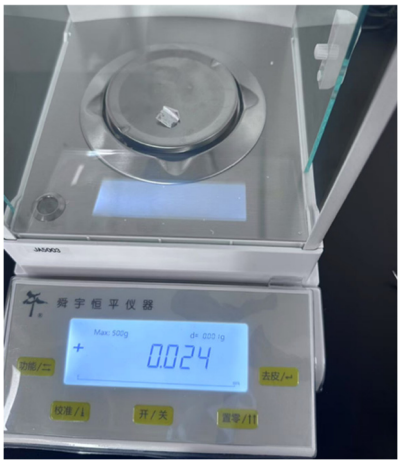


Figure 16. PVDF electrospun membrane after water absorption

By using an electronic scale, the mass of the sample before water absorption was 0.014g, and the mass after water absorption was 0.024g. Thus, it can be concluded that the water absorption rate of this sample is:

$$R_{PVDF} = \frac{0.024 - 0.014}{0.014} \times 100\% = 71.43\%$$

$$\Delta R_{PVDF} = \sqrt{\left(\frac{100 \cdot 0.024}{0.014^2} \times 0.001\right)^2 + \left(\frac{100}{0.014} \times 0.001\right)^2} \approx 14.18\%$$

$$R_{PVDF} = 71.43\% \pm 14.18\%$$

As shown in Figure 15 and 16, based on the measured data and error analysis of this experiment, the water absorption rates of all three samples were significantly higher than that of the PVDF hydrophobic control. Therefore, all three samples exhibited excellent water absorption capabilities. Among the three, sample 3 (15% PVA1750, pump speed 0.1 mL/h) outperformed samples 1 and 2 with an outstanding performance of 1300.0%1300.0%, and this conclusion was supported by both the smallest contact angle and the best SEM-preserved continuous porous structure.

4. Conclusion

In this study, three types of nanofiber membranes made

from chitosan were successfully prepared under different process conditions by electrospinning technology, and their properties were compared with those of polyvinylidene fluoride hydrophobic membranes (PVDF). Scanning electron microscopy observations revealed that sample 3 formed a continuous and uniform nanofiber network with intact pore structure and few spherical defects, which significantly enhanced the diffusion and absorption capabilities of liquids. Contact angle measurement results indicated that all three fiber membranes had good hydrophilicity, with sample 3 having the smallest contact angle and the strongest hydrophilicity. The water absorption test results further verified the correlation between morphology and performance. The water absorption rate of sample 3 was significantly higher than that of other samples and the control group.

The limitations of the experiment mainly lie in the relatively small dry weight of some samples, resulting in a relatively large relative error in water absorption rate calculation. At the same time, the practical parameter optimization range is limited, and the comprehensive influence of multiple factors such as concentration, pump speed, voltage, and humidity on the fiber morphology and performance has not been systematically explored. Moreover, the mechanical properties, long-term stability, and biocompatibility of the material have not been systematically evaluated.

In future experiments, increasing the sample quantity or increasing the number of parallel experiments to take the average value can be used to reduce measurement errors. At the same time, orthogonal experiments or response surface methods can be used to optimize the process parameters, and attempts can be made to improve the wet-state stability of the material through cross-linking or surface modification. In addition, the mechanical strength, breathability, antibacterial performance, and biocompatibility of the material can be tested to develop a sanitary pad material that is both highly absorbent, comfortable, safe, and biodegradable.

References

[1] Lasher, H. (2012). Publication: Bulletin of the World Health Organization; Type: Perspectives Article ID: BLT.12.110700.

[2] Sarah Fourcassier, Mélanie Douziech, Paula Pérez-López, Londa Schiebinger, Menstrual products: A comparable Life Cycle Assessment, Cleaner Environmental Systems, Volume 7, 2022,100096, ISSN 2666-7894

[3] Lasher, H. (2012). Publication: Bulletin of the World Health Organization; Type: Perspectives Article ID: BLT.12.110700.

[4] “Always Pads Testing Results.” Women’s Voices for the Earth, 10 Jan. 2020, womensvoices.org/menstrual-care-products/ detox-the-box/always-pads-testing-results/.

[5] Homa Homayoni, Seyed Abdolkarim Hosseini Ravandi, Masoumeh Valizadeh, Electrospinning of chitosan nanofibers: Processing optimization,Carbohydrate PolymersVolume 77, Issue 3, 2009, Pages 656-661, ISSN 0144-8617

[6] Sapkota S, Chou SF. Electrospun Chitosan-based Fibers for Wound Healing Applications. J Biomater. 2020 Dec;4(2):51-57. Epub 2020 Dec 4. PMID: 34056619; PMCID: PMC 8159176.

[7] Younes, I., & Rinaudo, M. (2015). Chitin and Chitosan Preparation from Marine Sources. Structure, Properties and Applications. Marine Drugs, 13(3), 1133-1174. https:// doi. org/ 10.3390/md13031133

[8] Sapkota S, Chou SF. Electrospun Chitosan-based Fibers for Wound Healing Applications. J Biomater. 2020 Dec;4(2):51-57. Epub 2020 Dec 4. PMID: 34056619; PMCID: PMC 8159176.